

Lattice field computations via recursive numerical integration

Tobias Hartung,^{a,b} Karl Jansen,^c Frances Y. Kuo,^{d,*} Hernan Leövey,^e Dirk Nuyens^f and Ian H. Sloan^d

^a*Computation-based Science and Technology Research Center, The Cyprus Institute, 20 Konstantinou Kavafi Street, 2121 Nicosia, Cyprus*

^b*Department of Mathematics, King's College London, Strand, London WC2R 2LS, United Kingdom*

^c*Deutsches Elektronen-Synchrotron DESY, Platanenallee 6, 15738 Zeuthen, Germany*

^d*School of Mathematics and Statistics, UNSW Sydney, Sydney NSW 2052, Australia*

^e*Structured Energy Trading, AXPO Trading & Sales, Parkstrasse 23, 5400 Baden, Germany*

^f*Department of Computer Science, KU Leuven, Celestijnenlaan 200A, 3001 Leuven, Belgium*

E-mail: tobias.hartung@desy.de, karl.jansen@desy.de, f.kuo@unsw.edu.au, hernaneugenio.leovey@axpo.com, dirk.nuyens@cs.kuleuven.be, i.sloan@unsw.edu.au

We investigate the application of efficient recursive numerical integration strategies to models in lattice gauge theory from quantum field theory. Given the coupling structure of the physics problems and the group structure within lattice cubature rules for numerical integration, we show how to approach these problems efficiently by means of Fast Fourier Transform techniques. In particular, we consider applications to the quantum mechanical rotor and compact $U(1)$ lattice gauge theory, where the physical dimensions are two and three. This proceedings article reviews our results presented in *J. Comput. Phys* 443 (2021) 110527 [17].

*The 38th International Symposium on Lattice Field Theory, LATTICE2021
26th–30th July, 2021
Zoom/Gather@Massachusetts Institute of Technology*

*Speaker

1. Introduction

Lattice Field Theory (LFT) serves as a non-perturbative tool to regulate Feynman's path integral, by removing infinities in the infra-red and ultra-violet. In LFT continuum models in physics are formulated on a finite Euclidean space-time lattice with lattice spacing h . In this way, an ultra-violet cut-off, $1/h$, is provided through a non-vanishing value of the lattice spacing. At the same time, the finite volume equips LFTs with an infra-red cut-off providing thus to a well-defined path integral, see e.g., [14] for an introduction to lattice field theories. (See [16, 22] for an alternative approach using the ζ -regularization.)

Another important aspect of Euclidean LFT is that the path integral and physical observables can be computed numerically within this framework. One very prominent example of a LFT is *Lattice Quantum Chromodynamics* (LQCD) which is the lattice version of *Quantum Chromodynamics* (QCD), the theory of the interaction between quarks and gluons. LQCD has been extremely successful in computing e.g., the low lying hadron spectrum, non-perturbative matrix elements and form factors, fundamental parameters of QCD and non-zero temperature physics, see e.g., the *Flavour Lattice Averaging Group* (FLAG) review [5].

The main tool for simulating LQCD are *Markov Chain Monte Carlo* (MCMC) methods such as Hybrid Monte Carlo, see [25] for an overview. The employed methods and algorithms have been immensely improved over the last years, leading to large factors of speedup in the numerical calculations. In addition, the structure of LQCD and of many other LFTs is of local nature, coupling essentially only nearest neighbours on the lattice. This allows for massively parallel simulations on state of the art supercomputers with (hundred) thousands of processors, which led to computations on lattices of size close to physical relevance, meaning that the first two quark generations, i.e., the up, down, strange and charm quarks, assume their physical values as determined from experiments.

Despite this enormous success, the MCMC approach is unable to address problems which lead to a complex integrand in the path integral, a situation which is referred to as *sign problem* [30]. These problems are of fundamental nature in the context of high energy physics. In particular, they are related to the questions: Why is there more matter than anti-matter in the universe? Why is there more experimentally detected CP violation than the standard model predicts? What are the physics of topological systems?

In addition, MCMC methods suffer from the problem of auto-correlations which is an inherent property of MCMC algorithms. This problem becomes severe when the continuum limit in LQCD is taken, i.e., when the lattice spacing is shrunk towards zero, see [2] and the references therein. In particular, it has been noticed [28] that the topological charge in LQCD starts to freeze in Monte Carlo simulations, making it thus very hard to take the continuum limit.

The above sketched shortcomings of MCMC methods has motivated researchers working in LFTs to constantly look for alternative approaches. The very large numerical demand of lattice simulations has triggered new approaches to accelerate LFT calculations even more and to achieve a very high accuracy in evaluating the path integral. The sign problem has led to new developments in using numerical techniques such as tensor networks [6] or tensor renormalization group methods [1].

In this proceedings article we report on a particular attempt to address the above mentioned problems by using efficient recursive integration techniques, combined with a Fourier analysis, following our original work in [17]. The idea is illustrated and applied to an abelian $U(1)$ compact

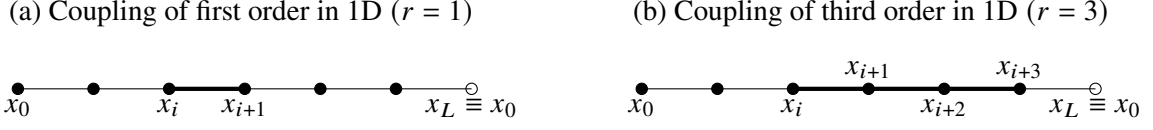


Figure 1: Different couplings in LQCD (Figure taken from [17, Fig. 1])

lattice gauge theory in two dimensions. By applying *lattice cubature rules* (see e.g., [12, 29]), the underlying group structure of this cubature allows for efficient computation when plugged into integrands exhibiting special structure as in the physics problems considered here. Although we will demonstrate the method here in two dimensions only, we see the prospect to generalize our method to higher dimensions and also to non-abelian groups in our future work.

To be more concrete, we will initially consider L -dimensional integrals (the “dimensionality” here refers to the number of integration variables rather than the space/time dimensions) of the form

$$\int_{D^L} \prod_{i=0}^{L-1} f_i(x_i, x_{i+1}) \, d\mathbf{x}, \quad \text{with } \mathbf{x} = (x_0, \dots, x_{L-1}) \text{ and } x_L \equiv x_0, \quad (1)$$

where each variable x_i belongs to a bounded domain $D \subset \mathbb{R}$ and each function f_i depends only on two consecutive variables x_i and x_{i+1} – which is called a *first order coupling* – and we implicitly assume periodic boundary conditions. Figure 1 sketches first order as well as third order coupling.

As already said above, we propose to solve lattice systems with such a coupling structure by approximating the involved integrals employing recursive numerical integration methods, where the lattice cubature rules used belong to a special family among *Quasi-Monte Carlo* rules (see e.g., [12, 13, 21, 24, 26, 27, 29]). The work we describe here is part of an ongoing effort by some of us to apply alternative to MCMC mathematical methods to tackle lattice models; previous works employ the Quasi-Monte Carlo approach [23], polynomially exact integration rules [4, 18], and a first applications of the recursive numerical integration technique to address quantum mechanical models [3, 17]. Quasi-Monte Carlo methods have also been considered in [9, 11] for multiloop calculations in perturbation theory.

In the next section we will provide the physical models considered. In the subsequent sections we will outline the efficient methods and the corresponding computational complexities. Executable Julia codes and numerical results can be found in the original work [17].

2. Description of physical models

In this section we will introduce the quantum mechanical rotor [3, 7, 8] and a 2-dimensional compact $U(1)$ lattice gauge theory, see e.g., [14] for an introduction into lattice field theories.

2.1 Quantum rotor

The quantum rotor is a quantum mechanical model which describes a particle with mass m_0 moving on a circle with radius r_0 , see e.g., [3, 7, 8]. We can supply the particle with a moment of inertia $I = m_0 r_0^2$. The quantum rotor can be formulated on a time lattice with lattice spacing $h = T/L$ between neighbouring lattice points, where T is the final time and L is the number of

lattice points. The variables of the system are taken to be angles $\phi_i \in D = [-\pi, \pi)$ defined at each time lattice point. In the continuum, the action of the system is given by

$$S(\phi) = \int_0^T \frac{I}{2} \left(\frac{d\phi}{dt} \right)^2 dt. \quad (2)$$

The discretized version of the action of the quantum rotor, using $\frac{1}{2} \left(\frac{d\phi}{dt} \right)^2 \approx \frac{1}{2} \left(\frac{\phi_{i+1} - \phi_i}{h} \right)^2 \approx \frac{1 - \cos(\phi_{i+1} - \phi_i)}{h^2}$, is then given by

$$S[\phi] = \frac{I}{h^2} \sum_{i=0}^{L-1} (1 - \cos(\phi_{i+1} - \phi_i))$$

and we impose periodic boundary conditions. The choice of the action will allow us to employ a combination of techniques as detailed below to make use of the Fast Fourier transform (FFT), reducing significantly the computational cost of the problem. As an observable we will take

$$O[\phi] = \cos(\phi_{k+1} - \phi_k) \quad \text{for any } k,$$

which is evaluated through the path integral as

$$\langle O[\phi] \rangle = \frac{\int_{D^L} \cos(\phi_{k+1} - \phi_k) \exp(\beta \sum_{i=0}^{L-1} \cos(\phi_{i+1} - \phi_i)) d\phi}{\int_{D^L} \exp(\beta \sum_{i=0}^{L-1} \cos(\phi_{i+1} - \phi_i)) d\phi}, \quad (3)$$

where $\beta = \frac{I}{h^2} = \frac{IL^2}{T^2}$. In order to evaluate the above integrals we will in the following convert their domain into the unit cube $[0, 1)^L$ since the integration domain $[0, 1)^L$ is the classical domain where Quasi-Monte Carlo rules are defined.

2.2 Quantum compact abelian gauge theory

Gauge theories are at the heart of the standard model of high energy physics. They are constructed such that they exhibit local gauge invariance, i.e., physical observables and the action of gauge models are invariant under local changes of the field variables defining a gauge theory. Using gauge invariant theories in constructing the standard model has been extremely successful. In particular, with the discovery of the Higgs boson, all particles predicted by the standard model have been identified experimentally. Thus, we now have a complete microscopic description of the interaction of the fundamental particles building all matter.

There are a number of non-perturbative aspects of gauge theories, such as confinement, topological effects and the existence of glueballs. The main tool, as formulated by Wilson [31] to understand these non-perturbative phenomena is *Lattice Gauge Theory* (LGT). On the lattice, the fundamental *gauge fields* are group valued and mainly taken from the abelian group $U(1)$, or the non-abelian ones, $U(N)$ or $SU(N)$ with $N \geq 2$.

Ideally, a study of gauge theories in three space and one time dimension (3 + 1 dimensions) would be preferable. However, this is presently not affordable within our approach and we therefore resort to a lower (1 + 1)-dimensional model, the (1 + 1)-dimensional compact $U(1)$ lattice gauge theory. The path integral of this model reads

$$\int_{D^{2L^2}} \exp \left(\beta \sum_{i=0}^{L-1} \sum_{j=0}^{L-1} \cos \left(\phi_{i,j}^a + \phi_{i+1,j}^b - \phi_{i,j+1}^a - \phi_{i,j}^b \right) \right) d\phi. \quad (4)$$

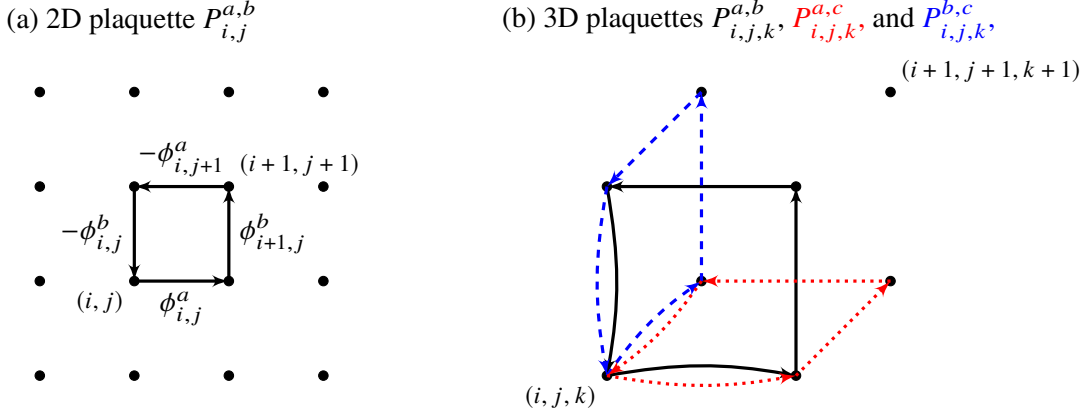


Figure 2: How to construct a plaquette in two and three dimensions (Figure taken from [17, Fig. 2])

In the two dimensional case, we construct the plaquette $P_{i,j}^{a,b}$ at lattice point (i, j) by carrying the field along the path $(i, j) \rightarrow (i+1, j) \rightarrow (i+1, j+1) \rightarrow (i, j+1) \rightarrow (i, j)$. The contribution of the angles ϕ is of positive sign if moving right or up, and the contribution is of negative sign if moving left or down. We index left/right movements with a superscript a and up/down movements with superscript b . For the three dimensional case, we add an extra forward/backward movement, which is denoted by the superscript c . This forms three independent smallest loops that can be taken: the (a, b) -plane (black solid line), the (a, c) -plane (red dotted line), and the (b, c) -plane (blue dashed line). One can see that each of these planes contribute equally with a “2-dimensional” plaquette. All visualized links are straight lines, they are only bent for better visualization.

Here $D = [-\pi, \pi]$, and we have parametric periodicity where all indices should be taken modulo L . A typical observable to be considered is the *plaquette expectation value*, see Figure 2(a),

$$\cos \left(\phi_{0,0}^a + \phi_{1,0}^b - \phi_{0,1}^a - \phi_{0,0}^b \right),$$

which we also study here.

The model above uses the plaquette – the smallest Wilson loop – to define the action. Alternative forms of the action, employing larger Wilson loops can be considered and are actually used in lattice simulations as they can improve the extrapolation behavior to the continuum limit, i.e., the limit where the lattice spacing is sent to zero. The only requirement is that these Wilson loops are gauge invariant and that the corresponding lattice action converges to the continuum action when the lattice spacing is sent to zero. Our method generalizes straightforwardly to such extended Wilson loops and in our original work [17] there is a detailed discussion of such a situation.

The construction of a $U(1)$ compact lattice gauge theory can be generalized to three dimensions as illustrated in Figure 2(b). The path integral then reads

$$\int_{D^{3L^3}} \exp \left(\beta \sum_{i=0}^{L-1} \sum_{j=0}^{L-1} \sum_{k=0}^{L-1} \left[\cos \left(\phi_{i,j,k}^a - \phi_{i,j+1,k}^a - \phi_{i,j,k}^b + \phi_{i+1,j,k}^b \right) \right. \right. \\ \left. \left. + \cos \left(\phi_{i,j,k}^c - \phi_{i+1,j,k}^c - \phi_{i,j,k}^a + \phi_{i,j,k+1}^a \right) \right. \right. \\ \left. \left. + \cos \left(\phi_{i,j,k}^b - \phi_{i,j,k+1}^b - \phi_{i,j,k}^c + \phi_{i,j+1,k}^c \right) \right] \right) d\phi,$$

while for the observable we again take the plaquette expectation value

$$O[\phi] = \cos\left(\phi_{0,0,0}^a - \phi_{0,1,0}^a - \phi_{0,0,0}^b + \phi_{1,0,0}^b\right).$$

In a more general way, the plaquette variable at a point (i, j) can be written as

$$P_{i,j}^{a,b} = \Phi_{i,j}^a \Phi_{i+1,j}^b (\Phi_{i,j+1}^a)^{-1} (\Phi_{i,j}^b)^{-1} \equiv e^{i(\phi_{i,j}^a + \phi_{i+1,j}^b - \phi_{i,j+1}^a - \phi_{i,j}^b)}. \quad (5)$$

This generalized form allows us to formulate the path integral and the gauge invariant observables by taking $\Phi_{i,j,\dots}^\alpha$ from $U(N)$ or $SU(N)$ and taking the trace as well as real parts of (5). For the physically relevant cases of the standard model, namely the weak interaction, or QCD (quantum chromodynamics or strong nuclear force), the relevant groups are $SU(2)$ and $SU(3)$, respectively.

3. Recursive numerical integration and complexity results

We present in this section a strategy to approximate the integral (1) using iterated integration and then replacing each of the iterated integrals by a numerical quadrature/cubature. We refer to this method as *recursive numerical integration*. The method first uses the fact that the integral (1) can be rewritten as

$$\begin{aligned} \mathcal{I} &= \int_D \cdots \int_D f_0(x_0, x_1) f_1(x_1, x_2) f_2(x_2, x_3) \cdots f_{L-1}(x_{L-1}, x_0) dx_0 \cdots dx_{L-1} \\ &= \int_D \left[\int_D \cdots \left(\int_D \left(\int_D f_0(x_0, x_1) f_1(x_1, x_2) dx_1 \right) f_2(x_2, x_3) dx_2 \right) \cdots f_{L-1}(x_{L-1}, x_0) dx_{L-1} \right] dx_0, \end{aligned} \quad (6)$$

with $\mathbf{x} = (x_0, \dots, x_{L-1})$ and $x_L \equiv x_0$. Due to the periodicity assumption of the indices of the variables, i.e., $x_L \equiv x_0$, we can start the iterated integration by choosing any variable of preference. The integrand presented here exhibits what is called a *first order coupling*, which means that each variable x_i is coupled via the physical model to its nearest neighboring variables x_{i-1} and x_{i+1} in a way that only these three variables are present in the iterated integration of the variable x_i .

Recursive integration has been considered in e.g., [10, 15, 19, 20], but not for integrands with parametric periodicity $x_L \equiv x_0$.

If we have an observable function that (i) depends only on one variable, or (ii) depends on two consecutive variables as in the factors f_i , or (iii) depends on many variables but takes the form of a product of first order couplings as for the integrand in (1), we will also arrive at an integral that can be expressed iteratively in the same manner as in (6). For all physical models considered in this proceedings article, we have observable functions that affect at most two consecutive variables (or can be decomposed into a direct sum of such functions) and therefore we can condense the effect of the observable function into a new integrand factor which, without loss of generality, can be included with the index 0 and be written as $f_0^\star(x_0, x_1) := O[x_0, x_1] f_0(x_0, x_1)$. In the coming sections, when the observable function is included in the integration, we will skip the \star notation and just mention that the integrand f_0 may be different from the other integrands f_i involved.

When the iterated integrals are replaced by the same approximating quadrature rule with points $t_0, \dots, t_{n-1} \in D$ and weights $w_0, \dots, w_{n-1} \in \mathbb{R}$, the resulting approximation scheme takes the form

$$Q = \sum_{k_0=0}^{n-1} w_{k_0} \left[\sum_{k_{L-1}=0}^{n-1} w_{k_{L-1}} \cdots \left(\sum_{k_2=0}^{n-1} w_{k_2} \left(\sum_{k_1=0}^{n-1} w_{k_1} f_0(t_{k_0}, t_{k_1}) f_1(t_{k_1}, t_{k_2}) \right) f_2(t_{k_2}, t_{k_3}) \right) \cdots f_{L-1}(t_{k_{L-1}}, t_{k_0}) \right]. \quad (7)$$

The recursive approximation procedure is then carried out as follows. Define M_i to be the $n \times n$ matrix with entries

$$(M_i)_{p,q} = f_i(t_p, t_q) \quad \text{for } p, q = 0, \dots, n-1, \quad (8)$$

and let W denote the $n \times n$ diagonal matrix with the weights w_0, \dots, w_{n-1} on the diagonal. Now we can express the innermost sum in (7) as

$$\begin{aligned} \sum_{k_1=0}^{n-1} w_{k_1} f_0(t_{k_0}, t_{k_1}) f_1(t_{k_1}, t_{k_2}) &= \sum_{k_1=0}^{n-1} (M_0)_{k_0, k_1} w_{k_1}^{1/2} w_{k_1}^{1/2} (M_1)_{k_1, k_2} \\ &= \sum_{k_1=0}^{n-1} (M_0 W^{1/2})_{k_0, k_1} (W^{1/2} M_1)_{k_1, k_2} = (M_0 W M_1)_{k_0, k_2}. \end{aligned}$$

Further we have

$$\begin{aligned} \sum_{k_2=0}^{n-1} w_{k_2} \left(\sum_{k_1=0}^{n-1} w_{k_1} f_0(t_{k_0}, t_{k_1}) f_1(t_{k_1}, t_{k_2}) \right) f_2(t_{k_2}, t_{k_3}) &= \sum_{k_2=0}^{n-1} w_{k_2} (M_0 W M_1)_{k_0, k_2} (M_2)_{k_2, k_3} \\ &= (M_0 W M_1 W M_2)_{k_0, k_3}. \end{aligned}$$

This leads to

$$\begin{aligned} Q &= \sum_{k_0=0}^{n-1} w_{k_0} (M_0 W M_1 W M_2 W \cdots M_{L-1})_{k_0, k_0} \\ &= \sum_{k_0=0}^{n-1} (W^{1/2} M_0 W M_1 W M_2 W \cdots M_{L-1} W^{1/2})_{k_0, k_0} \\ &= \text{trace}(B), \quad \text{with } B = W^{1/2} M_0 W M_1 W M_2 W \cdots M_{L-1} W^{1/2}. \end{aligned} \quad (9)$$

The equation (9) defines what we call the *recursive numerical integration* approach. It shows a clear advantage over the naive approach that could be used for approximation in (7) since the naive approach can be interpreted as a product rule over the L dimensional domain. If the quadrature rules has n points, this implies that the naive approach would have a cost equal to n^L , i.e., exponential in the dimension L . On the contrary, applying the recursive numerical integration approach we have an evaluation procedure for the approximation of the integral that reduces the complexity significantly and takes advantage of the particular structure of the matrices M_i . The matrix structure is of course a consequence of the structure of the underlying integrand factors f_i and the chosen quadrature rule.

Table 1 reviews the cases considered in the work [17] for different possibilities of matrices M_i one can find in LQCD applications.

There are particular conditions on the integrand and quadrature rule that lead to great improvements in terms of computational cost. In particular, if

1. each function f_i depends only on the difference of the two arguments, i.e., $f_i(u, v) = \kappa_i(v - u)$ for some function $\kappa_i : D \rightarrow \mathbb{R}$, and
2. each function κ_i is *periodic*, and
3. we have equally spaced points with equal weights $1/n$ (i.e., we have the rectangle rule),

then the matrix M_i is *circulant* and therefore FFT can be used to obtain the eigenvalues, see Scenarios (A5)–(A7) in Table 1.

If we replace the domain D in (1) by an s -dimensional domain D^s ,

$$\mathcal{I} = \int_{D^s} \cdots \int_{D^s} \prod_{i=0}^{L-1} f_i(\mathbf{x}_i, \mathbf{x}_{i+1}) \, d\mathbf{x}_0 \cdots d\mathbf{x}_{L-1}, \quad (10)$$

where $\mathbf{x}_i = (x_{i,0}, \dots, x_{i,s-1}) \in D^s$, with

$$x_{i,j} \equiv x_{i \bmod L, j \bmod s} \quad \text{for all } i, j \in \mathbb{N},$$

then the one-dimensional quadrature rule in (7) becomes an s -dimensional cubature rule with points $\mathbf{t}_0, \dots, \mathbf{t}_{n-1} \in D^s$ and weights $w_0, \dots, w_{n-1} \in \mathbb{R}$, and the matrices M_i in (8) become

$$(M_i)_{p,q} = f_i(\mathbf{t}_p, \mathbf{t}_q) \quad \text{for } p, q = 0, \dots, n-1.$$

Scenarios (A0)–(A4) from Table 1 apply again in this case. The following conditions are sufficient to ensure circulant matrices for the more favorable Scenarios (A5)–(A7):

1. each function f_i depends only on the difference of the two arguments, i.e., $f_i(\mathbf{u}, \mathbf{v}) = \kappa_i(\mathbf{v} - \mathbf{u})$ for some function $\kappa_i : D^s \rightarrow \mathbb{R}$, and
2. each function κ_i is *periodic with respect to each of the s components*, and
3. we have a *lattice cubature rule* with points

$$\mathbf{t}_k = \frac{k\mathbf{z} \bmod n}{n} \quad \text{for } k = 0, \dots, n-1,$$

and equal weights $1/n$.

A lattice cubature rule has an additive group structure. This means that the difference of two lattice points is another lattice point. Since the lattice cubature rule has equal weights $1/n$, we obtain circulant matrices M_i . This particular fact is the main motivation for favoring lattice cubature rules above all other cubature rules. The cost in all scenarios is *independent of s* . Nevertheless, the error is $O(n^{-\alpha})$, where α is determined by the cubature rule and the implied constant may depend on s .

Table 1: Recursive numerical integration for first order couplings (Table taken from [17, Table 1])

- M_i is the $n \times n$ matrix of f_i at quadrature points.
- W is an $n \times n$ diagonal matrix with quadrature weights on the diagonal.
- `eig` returns a diagonal matrix of eigenvalues.
- `fft` takes the first column of a circulant matrix and returns a diagonal matrix of eigenvalues.
- The quadrature error for all cases is $O(n^{-\alpha})$, with α given by the performance of the quadrature rule.
- The scenarios and strategies extend to an L -fold product of s -dimensional integrals with the quadrature rule replaced by an s -dimensional cubature rule. The cost remains independent of s . The error is again $O(n^{-\alpha})$, with α given by the performance of the cubature rule, and with an implied constant dependent on s .

Scenario	Strategy	Cost
(A0) naive implementation	$Q = \text{direct product calculation}$	n^L
(A1) recursive integration	$B = W^{1/2} M_0 W M_1 W \cdots M_{L-1} W^{1/2}$ $Q = \sum_{k=0}^{n-1} B_{k,k}$	$L n^3$
(A2) $M_i = M$	$A = W^{1/2} M W^{1/2}$ $B = A^L$ $Q = \sum_{k=0}^{n-1} B_{k,k}$	$\log(L) n^3$
(A3) $M_i = M$ diagonalizable	$A = W^{1/2} M W^{1/2}$ $\Lambda = \text{eig}(A)$ $Q = \sum_{k=0}^{n-1} \Lambda_{k,k}^L$	n^3
(A4) $M_i = M$ except M_0	$A = W^{1/2} M W^{1/2}$ $B = W^{1/2} M_0 W^{1/2} A^{L-1}$ $Q = \sum_{k=0}^{n-1} B_{k,k}$	$\log(L) n^3$
(A5) M_i circulant	$\Lambda_i = \text{fft}(M_i/n)$ for each i $Q = \sum_{k=0}^{n-1} \prod_{i=0}^{L-1} (\Lambda_i)_{k,k}$	$L n \log(n)$
(A6) $M_i = M$ circulant	$\Lambda = \text{fft}(M/n)$ $Q = \sum_{k=0}^{n-1} \Lambda_{k,k}^L$	$n \log(n)$
(A7) $M_i = M$ except M_0 all circulant	$\Lambda_0 = \text{fft}(M_0/n)$ $\Lambda = \text{fft}(M/n)$ $Q = \sum_{k=0}^{n-1} (\Lambda_0)_{k,k} \Lambda_{k,k}^{L-1}$	$n \log(n)$

These strategies have been extended in [17] to *higher order couplings* of order r , of the form

$$\begin{aligned} \mathcal{I} &= \int_{D^L} \prod_{i=0}^{L-1} f_i(x_i, x_{i+1}, \dots, x_{i+r}) \, d\mathbf{x} \\ &= \int_D \cdots \int_D f_0(x_0, x_1, \dots, x_r) f_1(x_1, x_2, \dots, x_{r+1}) \cdots f_r(x_r, x_{r+1}, \dots, x_{2r}) \\ &\quad \cdots f_{L-1}(x_{L-1}, x_0, x_1, \dots, x_{r-1}) \, dx_0 \cdots dx_{L-1}. \end{aligned}$$

The trick is to group successive r functions into a new factor to form a product of L/r factors (assuming for simplicity here that L is a multiple of r), and then apply the recursive strategies to these new factors. This yields analogous results to Scenarios (A1)–(A7), which are denoted by Scenarios (B1)–(B7) in [17, Table 2]. In all scenarios the error is again $\mathcal{O}(n^{-\alpha})$, with α determined by the quadrature/cubature rule, and the implied constant now depends on r .

4. Applications

In this section we consider applications of recursive numerical integration to the quantum rotor and the 2D compact $U(1)$ LGT problem. The interested reader can find numerical experiments for these two models in our recent work [17].

4.1 The Quantum rotor

For the quantum rotor, the integrals for the numerator and denominator of the normalized path integral ratio (3) are of the form

$$\int_{D^L} \prod_{i=0}^{L-1} f_i(x_{i+1} - x_i) \, d\mathbf{x},$$

where we have, after a change of variables, $D = [0, 1]$ and

$$f_i(x) = f(x) = \exp(\beta \cos(2\pi x)) \quad \text{for all } i = 0, \dots, L-1.$$

The only exception is that in the numerator integral we replace f_0 by

$$f_0(x) = \cos(2\pi x) \exp(\beta \cos(2\pi x)).$$

With a slight abuse of notation comparing with (6), here we have the (special) case $f_i(u, v) = \kappa_i(v - u) \equiv f_i(v - u)$, which means that each integrand factor $f_i(u, v)$ can be considered in fact as a function of one single variable by taking the difference of the two arguments u, v . The resulting functions $\kappa_i \equiv f_i$ are periodic and therefore we know that for the rectangle quadrature rule we have Scenario (A7) in Table 1, and thus the numerical integration cost becomes $\mathcal{O}(n \log(n))$.

The interesting case of higher order couplings for the quantum rotor arise when we consider higher order finite difference approximations of the physical discretization of the action in continuum (2). For example, the central difference formula $(-x_{i+2} + 8x_{i+1} - 8x_{i-1} + x_{i-2})/(12h)$ of order h^4 leads to (now with $\beta = IL^2/(144T^2)$)

$$\int_{D^L} \prod_{i=0}^{L-1} f(-x_{i+2} + 8x_{i+1} - 8x_{i-1} + x_{i-2}) \, d\mathbf{x},$$

which has order $r = 4$. This case can be solved using 4-dimensional lattice cubature rules combined with recursive numerical integration, following [17, Scenario (B4) in Table 2].

4.2 The 2D compact $U(1)$ lattice gauge theory model

Now we consider the model (4) which can be expressed in the generic form

$$\mathcal{I} = \int_{D^{L^2}} \int_{D^{L^2}} \prod_{i=0}^{L-1} \prod_{j=0}^{L-1} f_{i,j} \left(x_{i,j}^a - x_{i,j+1}^a - x_{i,j}^b + x_{i+1,j}^b \right) \mathrm{d}\mathbf{x}^a \mathrm{d}\mathbf{x}^b.$$

After a change of variables, we have $D = [0, 1]$ and

$$f_{i,j}(x) = f(x) = \exp(\beta \cos(2\pi x)) \quad \text{for all } i, j = 0, \dots, L-1.$$

To include the observable, in the numerator integral we will replace $f_{0,0}$ by

$$f_{0,0}(x) = \cos(2\pi x) \exp(\beta \cos(2\pi x)).$$

All these functions are clearly periodic. Below we will outline three stages to simplify the problem.

STAGE ONE

By rearranging the variables in the a -direction and the b -direction, we can write

$$\mathcal{I} = \int_{D^{L^2}} \prod_{i=0}^{L-1} \left(\underbrace{\int_{D^L} \prod_{j=0}^{L-1} f_{i,j} \left(x_{i,j}^a - x_{i,j+1}^a - x_{i,j}^b + x_{i+1,j}^b \right) \mathrm{d}\mathbf{x}_i^a}_{=: g_i(\mathbf{x}_{i+1}^b - \mathbf{x}_i^b)} \right) \mathrm{d}\mathbf{x}^b,$$

where we used the fact that each factor over the index i depends only on \mathbf{x}_i^a , and wrote the integral over $\mathbf{x}^a \in D^{L^2}$ as a product of integrals over $\mathbf{x}_i^a = (x_{i,0}^a, \dots, x_{i,L-1}^a) \in D^L$. This leads to

$$\mathcal{I} = \int_{D^L} \cdots \int_{D^L} \prod_{i=0}^{L-1} g_i(\mathbf{y}_{i+1} - \mathbf{y}_i) \mathrm{d}\mathbf{y}_0 \cdots \mathrm{d}\mathbf{y}_{L-1}, \quad (11)$$

where

$$g_i(\mathbf{y}) := \int_{D^L} \prod_{j=0}^{L-1} f_{i,j}(x_j - x_{j+1} + y_j) \mathrm{d}\mathbf{x}. \quad (12)$$

Thus we have obtained a nested integration problem where for the outer integral (11) we have an integrand with first order couplings of the form (10) (with s replaced by L), and for the inner integral (12) we have first order couplings given by (6) at each input i and \mathbf{y} . Then, the results in Table 1 apply for both the inner and outer integrals. If we use an n -point rectangle rule for the inner integral and an N -point lattice cubature rule for the outer integral, and if the functions $f_{i,j}$ are periodic (thus so are the functions g_i), then we will fall under Scenarios (A5)–(A7) for the inner and outer integrals. Furthermore, if all functions $f_{i,j}$ are the same, then the final cost is of order

$$N \log(N) + N n \log(n).$$

The cost is independent of L , while the error is of order $N^{-\alpha} + n^{-\alpha}$, with α given by the smoothness of the functions and the underlying lattice rule, with an implied error constant that may depend exponentially on L .

STAGE TWO

The next two lemmas show that the problem can be simplified further for this particular model with periodic functions $f_{i,j}$. The proofs can be found in [17].

Lemma 1 ([17]). *Assume the functions $f_{i,j}$ are periodic. Then the inner integral (12) simplifies to*

$$g_i(\mathbf{y}) = g_i\left(\sum_{j=0}^{L-1} y_j, 0, \dots, 0\right) = g_i\left(\sum_{j=0}^{L-1} y_j, \mathbf{0}\right), \quad (13)$$

that is, $g_i(\mathbf{y})$ depends only on the sum of the components of \mathbf{y} .

Lemma 2 ([17]). *Assume the functions $f_{i,j}$ are periodic. Then the outer integral (11) simplifies to*

$$\mathcal{I} = \int_{D^L} \prod_{i=0}^{L-1} g_i(y_{i+1} - y_i, \mathbf{0}) \, d\mathbf{y}. \quad (14)$$

The last transformation in Lemma 2 leaves the outer integral (14) in the form of (6) and so there is no longer a need to use a lattice cubature rule. By taking now an n -point rectangle rule for both the inner and outer integrals, Scenario (A7) applies in both cases and the cost becomes

$$n^2 \log(n).$$

The cost is again independent of L . The approximation error is then $O(n^{-\alpha})$, where α depends on the smoothness of the functions, but importantly, the implied constant no longer depends on L .

STAGE THREE

An alternative approach based on Fourier series was used in [17] to simplify the expression even further, as shown in the following theorem. The proof can be found in [17].

Theorem 1 ([17]). *Suppose that the functions $f_{i,j}$ are periodic and have absolutely convergent Fourier series. Define $\mu_{i+jL} := f_{i,j}$ for $i, j = 0, \dots, L-1$. Then the integral (11), with inner integral (12), simplifies to*

$$\mathcal{I} = \int_{D^{L^2}} \prod_{k=0}^{L^2-1} \mu_k(x_{k+1} - x_k) \, d\mathbf{x}, \quad (15)$$

where now the parametric periodicity is to be taken modulo L^2 , i.e., $x_k \equiv x_{k \bmod L^2}$.

Theorem 1 shows that, instead of nested integrals, we now have a single integral (15) with dimensionality L^2 of the form (6), with L replaced by L^2 . We are again in Scenario (A7) with an n -point rectangle rule and the cost is only of order

$$n \log(n),$$

and the error is $O(n^{-\alpha})$. Both the cost and the error bound are independent of L .

5. Summary

This proceedings article reviews our recent work published in [17]. We presented very high-dimensional integrals exhibiting a special structure, that arise from models such as the quantum rotor and the 2D compact $U(1)$ LGT. The numerical methods presented here and in [17] extend the ones presented in [3, 18]. In particular, here and in [17] we investigated in detail the advantages of applying FFT and gave sufficient conditions in order to meet the requirements of FFT application. The latter conditions may apply to other LQCD models than the ones presented in this work. Executable Julia codes were provided in [17] together with some numerical results.

The use of lattice cubature rules can be beneficial and even essential when we have an L -fold product of s -dimensional integrals, in order to meet the sufficient conditions to apply FFT. These improvements are not limited to systems with first order couplings. As shown in [17] they can be extended to systems with higher order couplings. In the latter case, the problems can still be truly high dimensional.

The application examples of the quantum rotor and 2D compact $U(1)$ LGT are encouraging us to look more deeply and to further investigate potential advantages on truly difficult problems in 3D and 4D compact $SU(N)$ LGT. We are currently investigating the latter problems using recursive numerical integration techniques.

Acknowledgments

We gratefully acknowledge financial support from the Australian Research Council (ARC) under grant DP210100831 and the Research Foundation Flanders (FWO) under grant G091920N.

References

- [1] S. Akiyama, Y. Kuramashi, and Y. Yoshimura, *Quantum field theories with tensor renormalization group*, arXiv:2111.04240 [hep-lat].
- [2] D. Albanea, P. Hernández, A. Ramos, and F. Romero-López, *Topological sampling through windings*, Eur. Phys. J. C **81** (2021), 873.
- [3] A. Ammon, A. Genz, T. Hartung, K. Jansen, H. Leövey, and J. Volmer, *On the efficient numerical solution of lattice systems with low-order couplings*, Comput. Phys. Commun. **198** (2016), 71–81.
- [4] A. Ammon, T. Hartung, K. Jansen, H. Leövey, and J. Volmer, *Overcoming the sign problem in one-dimensional QCD by new integration rules with polynomial exactness*, Phys. Rev. D **94** (2016), 114508.
- [5] S. Aoki *et al.* [Flavour Lattice Averaging Group], *FLAG Review 2019: Flavour Lattice Averaging Group (FLAG)*, Eur. Phys. J. C **80** (2020), 113.
- [6] M. C. Bañuls, K. Cichy, *Review on novel methods for lattice gauge theories*, Rept. Prog. Phys. **83** (2020), 024401.

- [7] W. Bietenholz, R. Brower, S. Chandrasekharan, and U. J. Wiese, *Perfect lattice topology: The Quantum rotor as a test case*, Phys. Lett. B **407** (1997), 283.
- [8] W. Bietenholz, U. Gerber, M. Pepe, and U.-J. Wiese, *Topological Lattice Actions*, JHEP **1012** (2010), 020.
- [9] S. Borowka, G. Heinrich, S. Jahn, S. P. Jones, M. Kerner, and J. Schlenk, *A GPU compatible quasi-Monte Carlo integrator interfaced to pySecDec*, Comput. Phys. Commun. **240** (2019) 120–137.
- [10] P. Craig, *A new reconstruction of multivariate normal orthant probabilities*, J. R. Statist. Soc. B **70** (2008), 227–243.
- [11] E. de Doncker, A. Almulih, and F. Yuasa, *High-speed evaluation of loop integrals using lattice rules*, J. Phys. Conf. Ser. **1085** (2018), no. 5, 052005.
- [12] J. Dick, F. Y. Kuo, and I. H. Sloan, *High-dimensional integration: the Quasi-Monte Carlo way*, Acta Numer. **22** (2013), 133–288.
- [13] J. Dick and F. Pillichshammer, *Digital Nets and Sequences*, Cambridge University Press, Cambridge, 2010.
- [14] C. Gattringer and C. B. Lang, *Quantum chromodynamics on the lattice*, Lect. Notes Phys. **788** (2010), 1.
- [15] A. Genz and D. K. Kahaner, *The numerical evaluation of certain multivariate normal integrals*, J. Comput. Appl. Math. **16** (1986), 255–258.
- [16] T. Hartung and K. Jansen, *Zeta-regularized vacuum expectation values*, J. Math. Phys. **60** (2019), 093504.
- [17] T. Hartung, K. Jansen, F. Y. Kuo, H. Leövey, D. Nuyens, and I. H. Sloan, *Lattice meets lattice: Application of lattice cubature to models in lattice gauge theory*, J. Comput. Phys. **443** (2021), 110527.
- [18] T. Hartung, K. Jansen, H. Leövey, and J. Volmer, *Avoiding the sign-problem in lattice field theory*, in Monte Carlo and Quasi-Monte Carlo Methods 2018 (B. Tuffin and P. L’Ecuyer, eds), Springer Proceedings in Mathematics & Statistics, vol 324, 2020, pp. 231–249.
- [19] A. J. Hayter, *Recursive integration methodologies with statistical applications*, J. Statist. Plann. Inference **136** (2006), 2284–2296.
- [20] A. J. Hayter, *Recursive integration methodologies with applications to the evaluation of multivariate normal probabilities*, J. Stat. Theory Pract. **5** (2011), 563–589.
- [21] F. J. Hickernell, *Lattice rules: How well do they measure up?*, in: Random and Quasi-Random Point Sets (P. Hellekalek and G. Larcher, eds.), Springer, Berlin, 1998, pp. 109–166.

- [22] K. Jansen and T. Hartung, *Zeta-regularized vacuum expectation values from quantum computing simulations*, PoS LATTICE **2019** (2020), 363.
- [23] K. Jansen, H. Leövey, A. Ammon, A. Griewank, and M. Müller-Preussker, *Quasi-Monte Carlo methods for lattice systems: a first look*, Comput. Phys. Commun. **185** (2014), 948–959.
- [24] C. Lemieux, *Monte Carlo and Quasi-Monte Carlo Sampling*, Springer, New York, 2009.
- [25] M. Lüscher, *Computational Strategies in Lattice QCD*, arXiv:1002.4232 [hep-lat].
- [26] H. Niederreiter, *Random Number Generation and Quasi-Monte Carlo Methods*, SIAM, Philadelphia, 1992.
- [27] D. Nuyens, *The construction of good lattice rules and polynomial lattice rules*, in: Uniform Distribution and Quasi-Monte Carlo Methods (P. Kritzer, H. Niederreiter, F. Pillichshammer, A. Winterhof, eds.), Radon Series on Computational and Applied Mathematics Vol. 15, De Gruyter, 2014, pp. 223–256.
- [28] S. Schaefer, R. Sommer, and F. Virotta [ALPHA], *Critical slowing down and error analysis in lattice QCD simulations*, Nucl. Phys. B **845** (2011), 93–119.
- [29] I. H. Sloan and S. Joe, *Lattice Methods for Multiple Integration*, Oxford University Press, Oxford, 1994.
- [30] M. Troyer and U.-J. Wiese, *Computational complexity and fundamental limitations to fermionic quantum Monte Carlo simulations*, Phys. Rev. Lett. **94** (2005), 170201.
- [31] K. G. Wilson, *Confinement of quarks*, Phys. Rev. D **10** (1974), 2445–2459.